Feature Article

Raman Microscopy Applied to the Development and Characterization of Next Generation Cutting-Edge Semiconductor Devices

Fran ADAR

Raman spectroscopy has been used since the early 1960's for the analysis of semiconductor materials, at a time when visible lasers became available and became the default source for Raman measurements. In the mid 1970's the Raman microscope was introduced[1]. Consequently as the integrated circuit business was developing, the application of Raman microscopy to the characterization of the materials for the analysis of device performance and engineering became important. Clearly applications to silicon were most relevant and included the measurement of stress, p-type doping (at high levels), crystallite size in polysilicon, and orientation as well as contaminant identification. In compound semiconductors more phenomena were explored. These included composition in alloyed semiconductors, doping of all types, and surface electrical fields which affect the doping and the depth of the surface depletion layer. Consequently, by tuning the excitation laser wavelengths different depths of the materials could be probed because of the dependence of the light penetration depth on wavelength. This enables differentiation of the characteristics of the surface depletion layer from the bulk. In this article we will review these effects historically in order to suggest how these phenomena can be pursued in wide bandgap semiconductors being developed for the next generation of devices. The article will also include a description of measurements on the nano scale, and the integration of photonics in integrated circuits.

Introduction

The title for this year's Masao Horiba Award was "Analysis and measurement technologies that contribute to the development of next-generation semiconductor devices." The next generation of semiconductor devices

1. will be continuing reduction of the size of the device structures below µm resolution,
2. will include optical integration on the integrated circuits, and

3. will include the use of high bandgap materials for high power applications.

Sub μm technology

Sub μm lithography developments go back at least to 1983 and were reviewed in 1986 when the field was still in the regime of university research[2]. The goal is to enable the production of a two-dimensional pattern of arbitrary structure with sharp sidewalls that are significantly smaller than what is possible with conventional optical methods that are determined and limited by the wavelengths of the light. Not only is the method of patterning the photoresist important but the ability of the photoresist itself to produce the desired pattern is considered. Several schemes for producing the lithographic images were reviewed in the above mentioned publication - optical projection photolithography, contact photolithography, holographic lithography, electron beam lithography, X-ray lithography, and ion lithography. Degradation of intensity contrast at the recording plane can result from diffraction, scattering, secondary electrons, penumbra, aberrations, distortions, etc. In addition, registration of subsequent masks can be a problem. This early work produced feature sizes of the order of 100 nm. Spatial resolution has been improved to better than 50 nm[3,4] using electron beam lithography and then 10 nm most recently[5]. For me tools of interference lithography are of particular interest because there are clever ways to pass coherent light through multiple transmission gratings and produce patterns. Interestingly, this technique depends on diffraction gratings with short pitches, fabricated from, for example, metals on Si_3N_4 membranes, materials very different from the gratings that we use in our instruments. As an example reference [4] discusses the use of electrohydrodynamic lithography (EHL) for sub-50 nm patterning and shows the successful use of a wedge geometry for varying hole patterns.

Figure 4 in that publication (reproduced here as Figure 1)

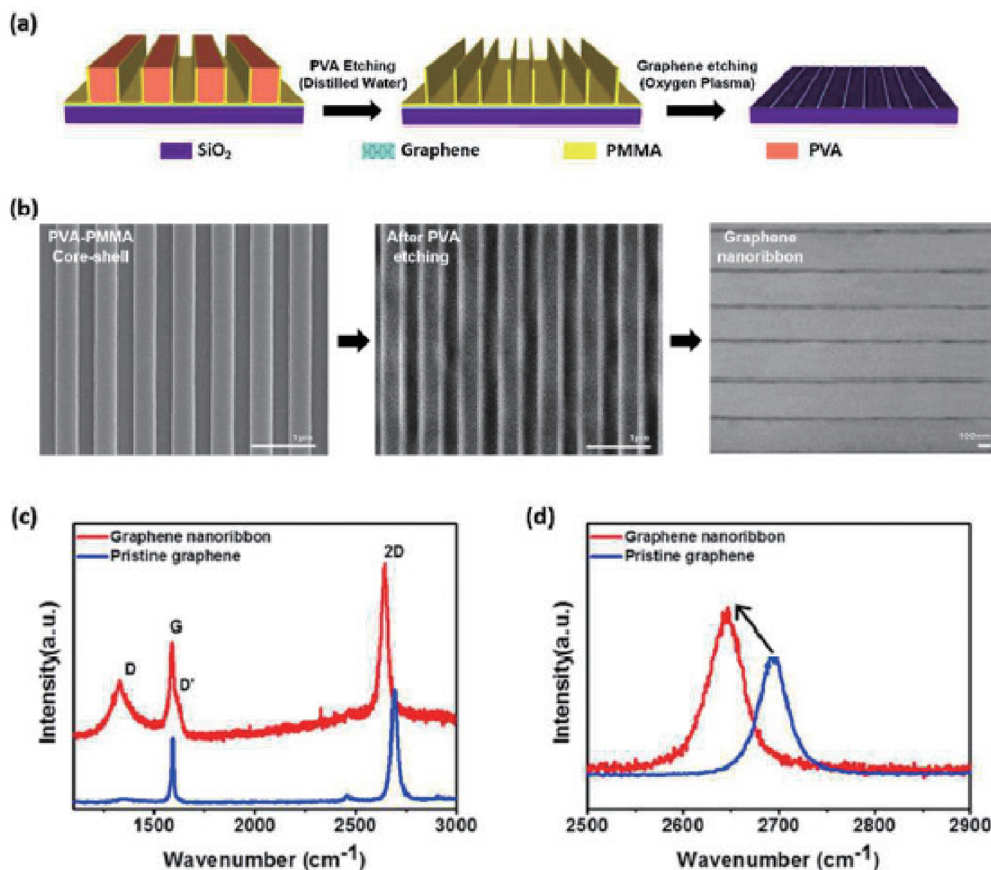

Figure 1 (a) Experimental procedure for the fabrication of a ~30 nm wide GNR array and (b) SEM images of the fabrication process for GNR's using core-shell-like nanostructures. (c) Raman spectra of pristine graphene and GNR's. D and D' bands appear in the GNR's. (d) 2D band is red-shifted owing to the strain in the GNR. Reproduced with permission from RSC Nanoscale 2017 00 1-3 Figure 4.

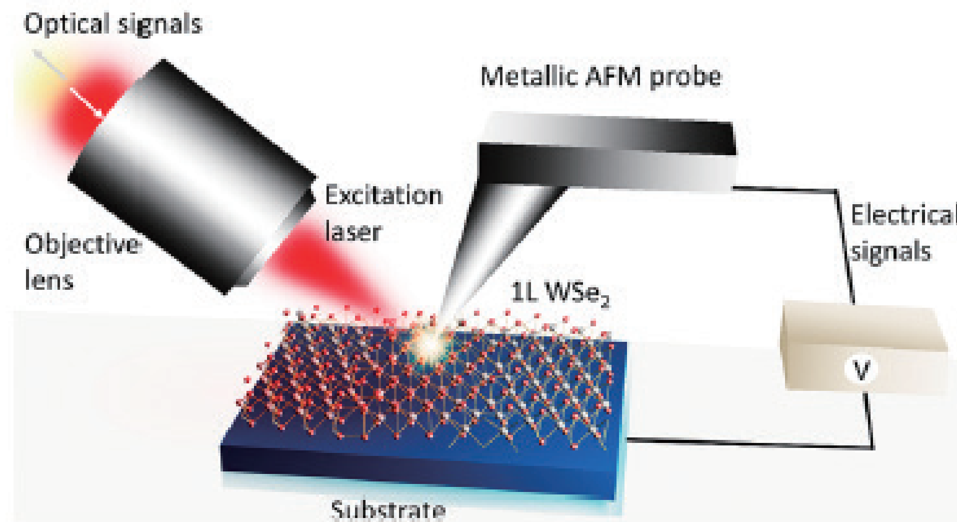

Figure 2 Experimental setup. Schematic diagram of the experimental setup used in the work of reference [8] to study the optoelectronic behavior of grain boundaries in 1L WSe2. *In situ* KPFM (Kelvin Probe Force Microscope) and TEOS (Tip Enhanced Optical Spectroscopy) measurements performed in the same experimental setup enable a direct correlation of topographical, excitonic, chemical, and electrical properties at the nanoscale. Reproduced with permission from W. Su, et.al, J. Phys. Chem. C 2021 125 26883 Figure 1.

shows the fabrication technology for a 30 nm wide graphene nano-ribbon (GNR) array. Note that the ability to fabricate this pattern depends on the properties of the polymer photoresist as well as the patterning technology. And the Raman spectrum indicates the nano-ribbon structure (by the presence of the D band) and strain (by the shift of the 2D band).

Nanoscale Raman microscopy

Since the mid 1970's the Raman microscope has been useful in analyzing spots as small as 0.5 µm in order to measure strain in silicon[6], and contaminating spots, among other things. In order to achieve comparable information on this nano-spatial scale, an AFM (atomic force microscope) coupled to a Raman microscope has been employed. Especially when TERS (tip-enhanced Raman spectroscopy) is employed, Raman signals from a region comparable to the size of the tip have been recorded[7]. While this reference [7] reviews much of the work until then (2013), it does not show spectra of silicon although it does treat carbon nanotubes and photovoltaic materials. One of the awardees at the Masao Horiba Awards was one of the earliest innovators of this technology[8] in which metal dichalcogenide (MDC) films were studied, and a Raman microscope with an AFM "accessory" is now commercially available from HORIBA. Note that in order to achieve nm scale resolution in the Raman analysis it is necessary to implement TERS. A typical scheme in which TERS is implemented for opaque materials is shown in Figure 2, which has been extracted from reference [8]. The excitation laser impinges on the sample from the side so that the AFM probe with a SERS-active coating (surface enhanced Raman spectroscopy) of silver or gold can be brought into close proximity to the surface. Typically measurements are made with the TERS probe close to the surface and then retracted; with the tip retracted the signal is the standard far-field signal, but with the probe close to the surface, the signal contains the near field contribution as well; the difference between the two signals is the TERS signal.

Because of the enhancement in carrier mobility when silicon is stressed, Si_xGe_{1-x} buffer layers were introduced to produce strain in silicon active layers and enable production of ultra-large integrated electronic circuits. But nanoscale fluctuations in the strain distribution were known to reduce the performance of the devices. Consequently, there was interest in recording Raman spectra on the nm scale in order to control the device quality. TERS Raman signals from strained silicon were reported in 2007[9]. Figure 3 is reproduced from that publication and the spatial resolution, in nm rather than µm, was determined by the diameter of the tip.

The following paragraphs describe various phenomena in silicon that can be studied by Raman and followed on the nm scale with TERS.

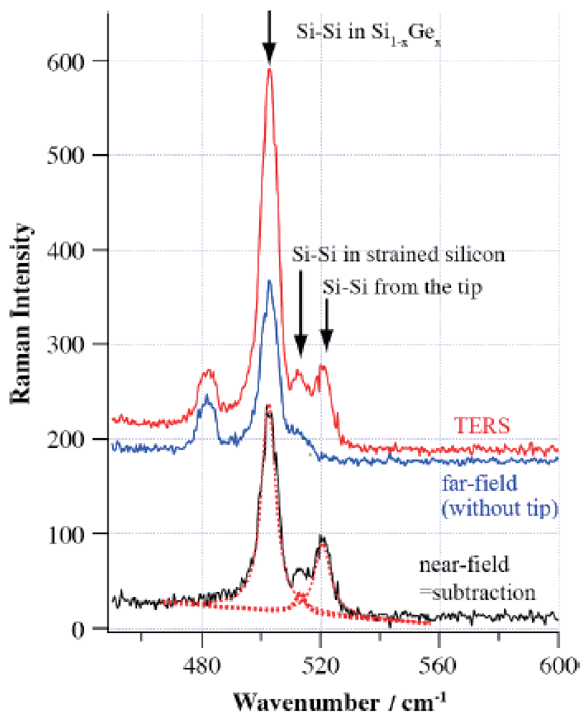

Figure 3 TERS spectra of strained silicon and the far-field spectrum. The black line is the subtracted spectrum (near-field spectrum) between TERS and far-field spectrum. Dotted lines are the Lorentzian curve-fitting for the near-field spectrum. Reproduced with permission from N. Hayazawa, et.al,. J. Raman Spectrosco 2007 38 684 Figure 6.

Group IV Semiconductors, especially Si

With lasers in the visible part of the spectrum, scattering is always done in the back-scattering configuration, and this is always the case when using a microscope for excitation. In Si, one can monitor the orientation (using polarization conditions), strain (by measuring spectral shift due to the geometry of the integrated circuit), crystallite size in polysilicon (by measuring spectral shift and linewidth), and temperature (by taking the ratio of the anti-Stokes to Stokes scattering). Information on this can be found in references [6 and 9].

There is one more phenomenon seen in silicon that is rather interesting and potentially useful. When Si is heavily doped with ions producing p-type doping, there are possible electronic transitions between levels of the valence band. Because these transitions are of the order of 500 cm^{-1} which is a value quite close to the phonon value, there is an interaction called the Fano interaction which describes coupling between a state with a narrow set of values (the phonon) and a continuum of states with a larger set of values (the electronic transitions). This phenomenon has been known in Si for many years, and the result is a distorted lineshape of the phonon[10]. Figure 4 is reproduced from reference 10 (Figure 2). The authors even discuss how Raman measurements can be used for diagnostics of doping in circuits as they are being fabricated.

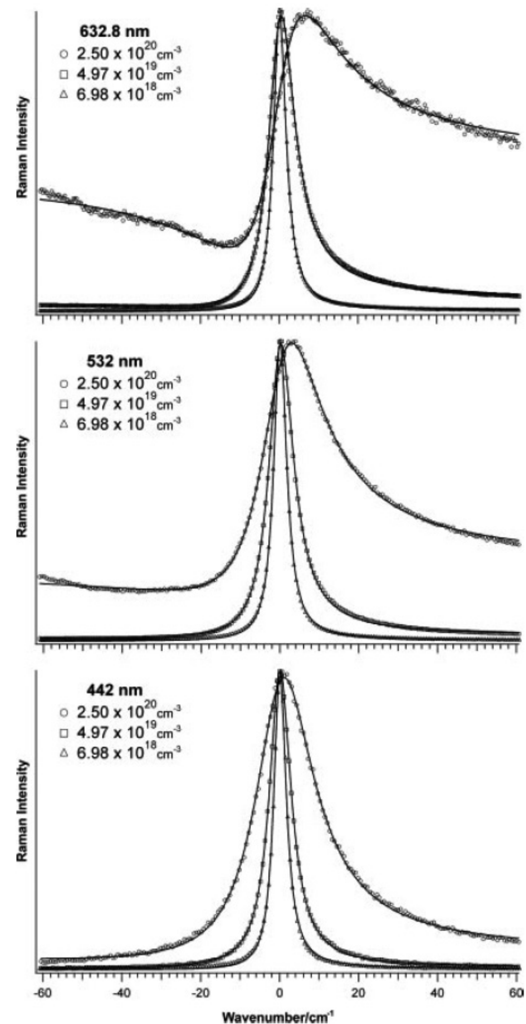

Figure 4 Raman lineshapes versus scattering wavelength for three thermally diffused boron doped Si(100) samples at excitation wavelengths 632.8, 532, and 442 nm. The experimental data (discrete points) were fitted with the modified Fano function (solid lines) with a least-squares computer fit which used q and Γ as adjustable parameters, defined in the reference. The spectra were normalized by the maximum peak value of each concentration. Reproduced with permission from B.G. Burke, et.al., Raman study of Fano interference in p-type doped silicon J Raman Spectrosc. 2010 41 1759-1764 - Figure 2.

The other Group IV semiconductor of interest is Ge. Even though the first transistor was made in Ge before 1950, since about 1960 all commercial transistors have been based on Si. That is until SiGe has been implemented. SiGe introduces strain which enhances carrier mobility, provides the ability to engineer the bandgap and to integrate CMOS logic with heterojunction bipolar transistors allowing it to be used on mixed signal integrated circuits for applications such as telephones[11]. In principle the frequency of the Raman bands should enable one to calculate the composition, but in this system, strain induced by the differences in atomic size and interatomic spacings also cause spectral shifts. However, using polarization

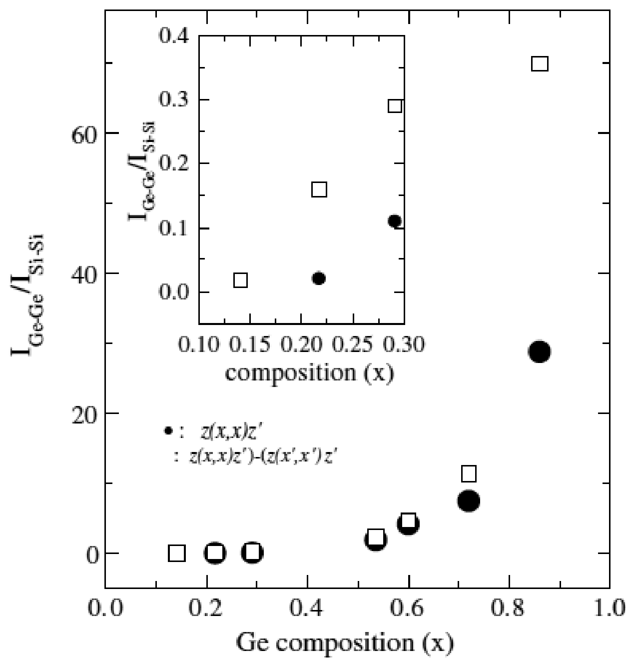

Figure 5 Calibration curve for x, the proportion of Ge in a SiGe alloy, based on I_{Ge-Ge}/ I_{Si-Si} ratio obtained from curve-fitting of the unsubtracted: z(x.x)z' ● and subtracted: [z(x.x)z']-[z(x',x')z'] □ spectra. Reproduced with permission from S. Rath, et. al,. Semicond. Sci. Technol. 2003 18 566 Figure 10.

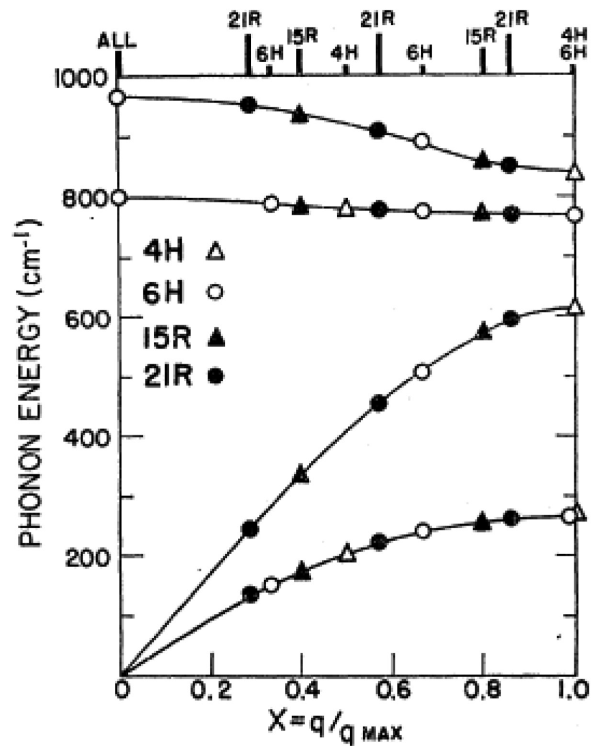

Figure 6 Combined dispersion curves using data from four polytypes. For each polytype, the Raman accessible values of $x=q/q_{max}$ are marked at the top of the figure. Reproduced with permission from D.W. Feldman, et.al., Phonon Dispersion Curves by Raman Scattering in SiC, Polytypes 3C, 4H, 6H, 15R and 21R Phys. Rev. 1968 173 3 787-793.

measurements to separate the various effects, a calibration protocol based on intensities was established[12]. Figure 5 shows the calibration curve of Ge in Si.

Before leaving this review of Group IV semiconductors, there is another system that has to be mentioned. SiC is analogous to silicon, germanium, and diamond, except that one atom in the cubic unit cell is Si while the second is C. Like silicon, germanium and diamond, it is also an indirect gap material (E_g ~3eV) making it one of the wide bandgap materials that will be exploited in the next generation of semiconductor devices; its large bandgap makes it a good substrate for working at higher temperatures and consequently higher power.

SiC actually occurs in many polytypes that are related to each other by systematic rotations around the (111) axis of the cubic phase. The Raman spectra of these materials are quite interesting, and it is not difficult to differentiate them[13]. Figure 6 is extracted from reference 13 and represents a consolidated dispersion curve for several polytypes. The X axis corresponds to the Brillouin zone of the cubic polytype. For each of the other polytypes the Brillouin zone of the cubic phase is folded to accommodate the number of layers in the identified phase. H indicates a hexagonal phase and R indicates a rhombohedral phase. The mode derived from the cubic TO for all polytypes is close to 800 cm^{-1} and would not easily enable identification. The mode derived from the cubic LO mode does vary from about 970 to 830 cm^{-1}, but it can also be affected by doping[14]. Graded doping was used to study the interaction between carrier transport and phonon properties; it was shown that line shape analysis provided information on the damping of free carriers as well as carrier concentrations. The effects of doping in SiC are analogous to those in III-V semiconductors which will be discussed in the following section. (The meaning of TO, transverse optical, and LO, longitudinal optical, modes will become clear in the next section on III-V semiconductors.) However, the folded acoustic modes, especially the LA (longitudinal acoustic) mode varies quite a bit in the different polytypes, in Figure 6 between about 240 and 600 cm^{-1}. Because of the ability to form polytypes easily by rotations around the cubic (111) axis, defects are common in engineered materials[15] and can be analyzed by their Raman spectra. This is actually discussed in detail in reference 15. The effects of strain[16] in SiC have also been documented.

III-V Semiconductors

While the longitudinal and transverse optical phonons in Group IV semiconductors (Si, Ge, and Diamond) are degenerate (ie,. they have the same energy), in III-V semiconductors the two are split because of the electric field that the inequivalent ions create during vibrational

motion. A good reference for many semiconductor materials is the European Commission's "Nostradamus" project[17]. From this reference the LO (longitudinal optical) and TO (transverse optical) frequencies of most of the semiconductors of interest can be found.

There is another effect in III-V semiconductors that results from the fact that free electrons from doping can shield the electric field of the LO phonons[18]. In fact, the free electrons form a plasmon in the material and the plasmon interacts with the LO phonon producing the L_+ and L_- modes seen on the left side of Figure 7. When the density of free electrons is very high, the frequency of the L_- phonon collapses to that of the TO phonon and the frequency of the L_+ plasmon follows the trajectory of a free plasmon. The next figure, reproduced from reference 18 shows the spectrum of a GaAs sample doped at 1.9×10^{18} cm^{-3} (left, for different polarization conditions) and then the dependence of the energies of the LO phonon and plasmon on the square route of the dopant levels (right). This is the earliest measurement of the coupled LO phonon-plasmon modes of which I am aware. Note that the measurement was made with a Nd:YAG laser whose emission wavelength is below that of the bandgap; the measurements were made in the bulk and avoided surface field effects.

When using a visible laser investigating III-V semiconductors, the depth of penetration of the laser and the thickness of the surface depletion layer will affect these measurements. Much of the information necessary for design and interpretation of such measurements are available in reference [17].

Semiconductor engineers often are interested in tuning the properties of semiconductors for devices by alloying materials that have (almost) equal interatomic spacings; $In_xGa_{1-x}As$ is a good example. The reason to select a pair with almost equal interatomic spacings is to minimize strain and to maintain single crystal structure, ie,. minimize dislocations and avoid cracking. There is a good reference that discusses how alloying affects the phonons[19]. By alloying, the engineer can tailor the bandgap for a particular application. For instance, communication lasers use a bandgap that matches the wavelength where fiber optics that carry the laser signals have minimum losses (1.5 µm), and InGaAsP is used in the design of the laser.

In understanding the observed phonon behavior of III-V alloys there are two possibilities - two- mode and one-mode behavior. Figure 8 reproduces the behavior for the two types of mixed phonons and is reproduced from reference [19].

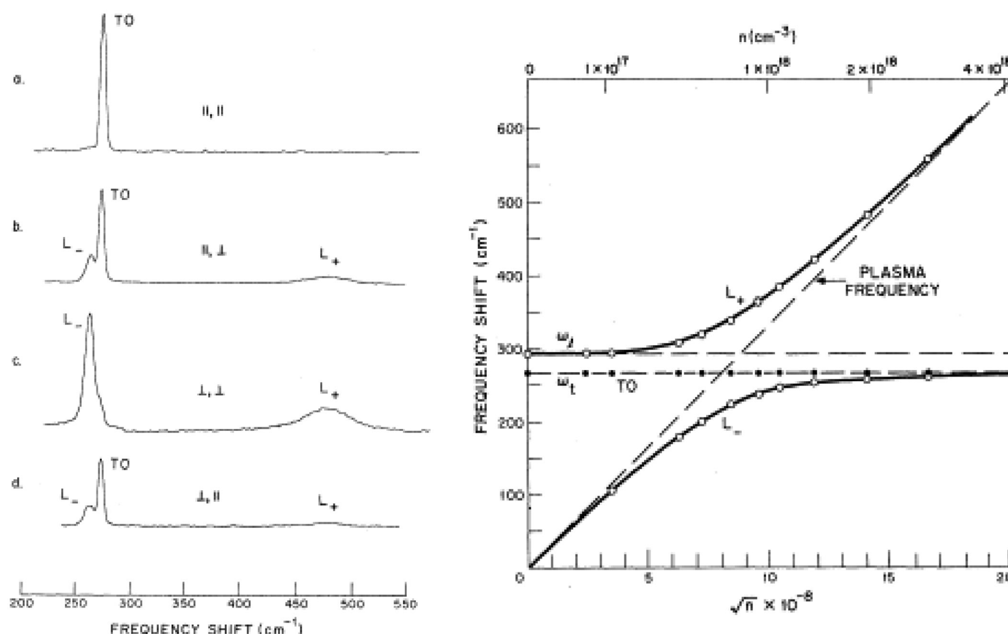

Figure 7 Left: Intensity and polarization properties of the Raman-scattered light from GaAs at liquid He temperature for a sample with $n=1.9 \times 10^{18}$ cm^{-3}. The scattering angle is 90° with the incident and scattered light propagating along a (100) direction. The || and | symbols indicate the polarization of the incident and scattered light with respect to the plane of scattering. These traces are uncorrected for the system response, and the gain in b is lower than the others. Right: Frequencies of the L_+ and L_- modes (mixed longitudinal phonon-plasmon modes) as a function of the square root of the carrier concentration. Reproduced with permission from A. Mooradian and A.L. McWhorter 1967, Polarization and Intensity of Raman Scattering from Plasmons and Phonons in Gallium Arsenide Phys. Rev. Let. 19 15 849-852 Figures 1 and 2.

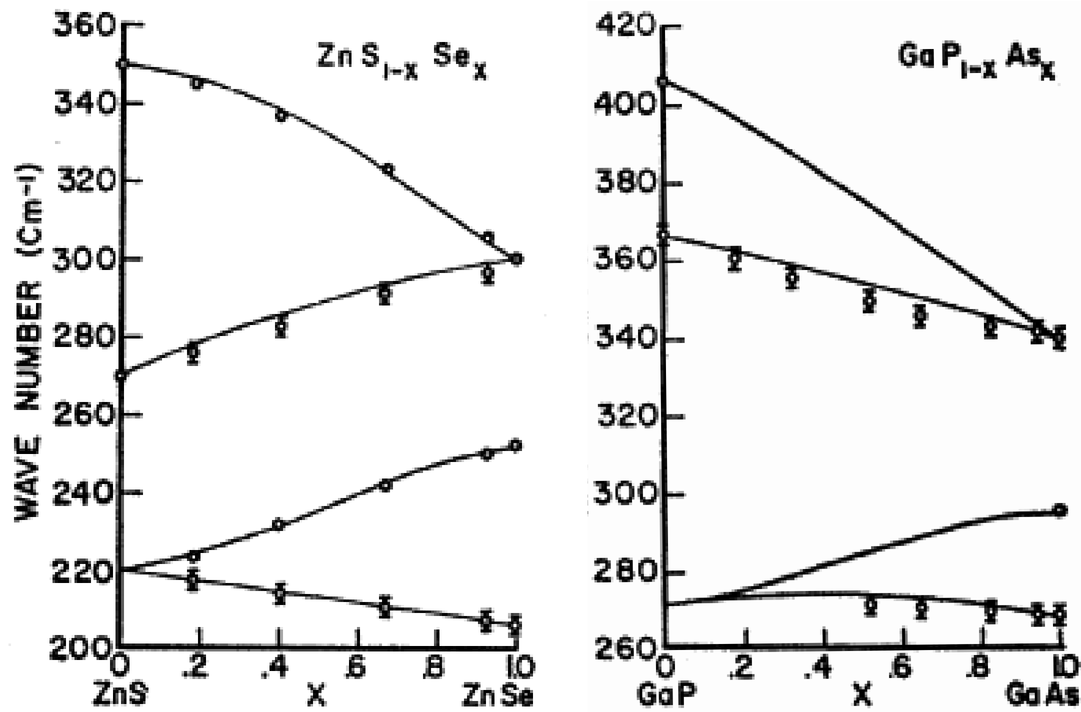

Figure 8 Left: Two mode behavior in ZnS_{1}-xSe_{x}. The open circles O represent the measured LO phonons and Φ represents the measured TO phonons. Right: One Mode Behavior in $GaP_{1-x}As_{x}$. The solid lines in the figures, ——— indicate theoretical predictions explained in the publication. Reproduced with permission from I.F. Chang and S.S. Mitra. Application of a Modified Random-Element-Isodisplacement Model to Long-Wavelength Optic Phonons of Mixed Crystals Phys Rev 1968 172 3 924-933 Figures 2 and 3.

In both figures the measured phonon frequencies at the endpoints represent the pure materials. In the two-mode behavior of $ZnS_{1-x}Se_{x}$ at any x different from 0 or 1 there is a set of LO and TO phonons whose behavior represents a mixture of the two pure materials. In the one mode behavior of $GaP_{1-x}As_{x}$ there is only one TO mode and one LO mode for any value of x. The cited reference [19] describes the origins of these differences.

There is another phenomenon that the analyst needs to keep in mind. Because of pinning of electronic states at the surfaces of doped III-V semiconductors there is a layer depleted of electrons. Consequently if one measures a Raman signal with a laser that does not penetrate deeper than that surface depletion layer, the LO phonon frequency will reflect a carrier-free material. If a longer wavelength laser is used that does penetrate through the surface depletion layer, then the contributions to the scattering from that region will reflect the carrier concentration. The wavelength dependence of the absorption region and a means to calculate the space charge layer are included in reference [17].

Transition metal dichalcogenides

Probably the most exciting and active area in semiconductor research now is that of the transition metal dichalcogenide (TMD) films. Because of the potential to tailor their electronic and optical properties they are being considered for design into the next generation of devices. Raman microscopy, including TERS, provides the ability to observe the effects of crystal edges and internal twin boundaries with up to ~15 nm spatial resolution, correlating spectral shifts with PL (photoluminescence intensity) and the exciton diffusion length[20].

Optical Integration on Integrated Circuits

The next generation of technology will make use of chips that integrate photonics with electronics in order to increase speed of data transfer, speed of calculations, simplify design, and reduce energy consumption. The goal is to perform all functions on a silicon substrate. But a major hurdle is the intrinsic characteristic of silicon, that it is an indirect gap material and therefore is not an immediate choice for light generation. In addition, the integration of materials not normally used on a silicon integrated circuit (IC) will also be a challenge.

While a final solution for full integration is not yet available, considerable strides have been made, and are reviewed in a 2024 publication[21]. The ultimate goals include the ability to fabricate in silicon foundries, to shrink the chips, to increase the number of devices that can be integrated on a chip, and to minimize power consumption. Currently photonic integrated chips are dominated by communications applications, but it is foreseen that such technology can accommodate quantum

computing and sensors, especially for biomedical application, while photonics provides data links, electronics control readout and digital signal processing. Because photons do not interact with each other, they transmit information with fidelity, but electrons do interact and can therefore be used for switching and computing. On the other hand, silicon photonics carrier waves are in the 100's of THz range whereas silicon electronics are in a range less than THz. Hurdles to be overcome include: Hurdles to be overcome include:

- identifying an appropriate laser source. If it will be something like InAsP, it has to be incorporated on the chip, and possibly designed as a comb for multiwavelength output

- designing the I/O for the photonics and incorporating them on the chip.

- designing high confinement waveguides for modulation, integrating Wavelength Division Multiplexer (WDM) (for disentangling parallel transmission of multiple signals over different wavelengths) and incorporating focal plane array detector systems in order to detect simultaneously the various channels.

- Incorporating Si/Ge avalanche photodiodes (APD's).

- integrating a variety of dissimilar materials.

Raman microscopy can assist in analyzing materials in all of the above. In addition to the excellent review of the engineering challenges described in reference [21] there are some developments that are worthy of note.

In 2004 it was reported that full optical control of light on a silicon chip was achieved by using an "all-optical gate based on a silicon micrometer-size planar ring resonator" operator with low pump-pulse energies[22]. A continuous wave laser was produced on silicon in 2005[23] by launching a pump laser into a low-loss silicon-on-insulator rib waveguide by using a p-i-n structure on either side of the waveguide to reduce the two-photon absorption losses due to free carriers. The origin of the lasing was the stimulated Raman signal of the silicon of the waveguide. Note that this design requires a pump laser so the requirement for non-silicon materials is not eliminated.

Another innovation of note is inclusion of a Mode Division Multiplexer (MDM) in addition to the WDM; the MDM independently separates spatial modes of each wavelength and ultimately provides a multiplicative effect on the bandwidth of the optical link. Chip to chip transmission was demonstrated between separate silicon chips[24]. For sure there are, and will continue to emerge, new technologies that will further enable integrated electronics/photonics.

Next Generation Semiconductor Devices; Analysis by Raman Microscopy

The potential of Raman microscopy to the analysis and characterization of the next generation of semiconductor devices requires an understanding of what type of information Raman spectroscopy can provide. This required an extensive review of the contributions of Raman spectroscopy to the analysis of classical semiconductors and which appeared earlier in this document.

One of the most important areas for the future of semiconductor devices is the use of high bandgap semiconductors for high power applications such as for electrical vehicles. This would include SiC, GaN or AlN, and Ga_2O_3. The last one is surprising because until now oxides have been considered insulators but the ability to fabricate field effect transistors has been demonstrated[25]. Polarized Raman spectra from single crystals of Ga_2O_3 have been recorded so it can be assumed that Raman is available for analysis of this material as well[26].

As was stated earlier in this document, work on thin layer metal dichalcogenides is active because of the potential to tune their properties which will provide new capabilities in devices (20). And the article cited above shows a clear path between Raman analysis and electronic properties.

In considering the production of nano-sized electronic devices, we should mention the potential of optical metasurface engineering for large scale production of devices with sub 50 nm scale in silicon foundaries. This is currently not a reality but is certainly being pursued (reference [21]).

One last area to be mentioned is the re-engineering of packaging to accommodate the coming requirements for performance, power (heat dissipation), and cost[27]. The trend is seen to be moving from polymeric materials to inorganic materials such as silicon and ceramics in addition to metals for the interconnects. Note that the Raman spectra of ceramics[28] are strong and quite diagnostic of crystallographic phase (which determines the properties of the materials) making Raman an appropriate analysis method.

Conclusion

Raman analysis of semiconductors goes back at least to the late 1960's, about the time that lasers first became available as excitation sources. The wealth of information and effects documented over the years provide fertile ground for the use of Raman microscopy in the design, characterization, and analysis of next generation devices. The phenomena that are amenable to detection by Raman microscopy are well known so it will be straightforward to know how the technology can aid in the characterization of devices under development - whether that means measuring strain produced by the materials used or the local geometry of the device, or measuring composition of alloyed materials (SiGe or III-V semiconductors), or measuring the effects of free carriers which determine device performance. While proof of concept for these innovations is ongoing both in industry and academia, national efforts such as the Chip Act in the United States indicates the high level of awareness for the need for investment.

* Editorial note: This content is based on HORIBA's investigation at the year of issue unless otherwise stated.

References

[1] George Turrell and Jacques Corset. Raman Microscopy Developments and Applications Academic Press London (1996) and references therein that describe the original publications

[2] H.I. Smith. A Review of Submicron Lithography. 1986 *Superlattices and Microstructures* 2 2 129-142

[3] A. Kojima, H. Ohyl, and N. Koshida Sub-50 nm resolution surface electron emission lithography using nano-Si ballistic electron emitter 2008 J *Vac Sci Technol* B 26 6

[4] S. Lee, et.al. Innovative Scheme for Sub-50 nm Patterning via Electrohydrodynamic Lithography 2017 RSC *Nanoscale* 00 1-3 1-7

[5] N.Mojarad, J. Gobrecht, and Y Ekinci Interference lithography at EUV and soft X-ray wavelengths: Principles, methods, and applications 2015 *Microelectron Eng* 143 55-63

[6] I. De Wolf. H. Norstrom. And H.E. Maes, Process-induced mechanical stress in isolation structures studied by micro-Raman spectroscopy, 1993 J *Appl Phys* 74 7 4490-4500

[7] T. Schmid. L. Opilik. C. Blum. And R. Zenobi, Nanoscale Chemical Imaging Using Tip-Enhanced Raman Spectroscopy: A Critical Review *Angew. Chem. Int. Ed.* 2013 52, 5940-5954

[8] W. Su, N. Kumar, H. Shu, O. Lancry and M. Chaigneau *In Situ* Visualization of Optoelectronic Behavior of Grain Boundaries in Monolayer WSe_2 at the Nanoscale J *Phys Chem* C 2021 125 26883-26891

[9] N. Hayazawa, et.al, Viualization of localized strain of a crystalline thin layer at the nanoscale by tip-enhanced Raman spectroscopy and microscopy, *J. Raman Spectrosc* 2007 38 684-696

[10] B.G. Burke, et.al., Raman study of Fano interference in p-type doped silicon *J Raman Spectrosc*. 2010 41 1759-1764

[11] Silicon-germanium - Wikipedia

[12] S. Rath, M.L. Hsieh, P. Etchegoin, and R.A. Stradling Alloy effects on the Raman spectra of $Si_{1-x}Ge_x$ and calibration protocols for alloy compositions based on polarization measurements 2003 *Semicond. Sci. Technol.* 18 566-575 2003

[13] D.W. Feldman, et.al, Phonon Dispersion Curves by Raman Scattering in SiC, Polytypes 3C, 4H, 6H, 15R, and 21R *Phys. Rev.* 1968 173 3 787-793

[14] S. Nakashima, et.al., Raman scattering study of carrier-transport and phonon properties of 4H-SiC crystals with graded doping, *Phys Rev.* B 76 2007 245208

[15] P-C Chen. et.al., Defect Inspection Techniques in SiC, *Nanoscale* Res ett 2022 17:30

[16] W.L. Zhu. J.L. Zhu, S. Nishino and G. Pezzotti, Spatially resolved Raman spectroscopy evaluation of residual stresses in 3C-SiC layer deposited on Si substrates with different crystallographic orientations *Appl Surface Sci* 2006 252 2346-2354

[17] Raman and Luminescence Spectroscopy for Microelectronics ISBN 92-828-5011-0

[18] A. Mooradian and A.L. McWhorter 1967, Polarization and Intensity of Raman Scattering from Plasmons and Phonons in Gallium Arsenide *Phys. Rev. Let.* 19 15 849-852

[19] I.F. Chang and S.S. Mitra. Application of a Modified Random-Element-Isodisplacement Model to Long-Wavelength Optic Phonons of Mixed Crystals *Phys Rev* 1968 172 3 924-933

[20] K-D Park, et.al, Hybrid Tip-Enhanced nanospectroscopy and Nanoimaging of Monolayer WSe2 with Local Strain Control *Nano Lett* 2016 16 2621-2627

[21] S. Shakhar, et.al,. Roadmapping the next generation of silicon photonics *Nature Commun* 2024 15.751

[22] V.R. Almeda, C.. Barries, R.R. Panepucci and M. Lipson, All-optical control of light on a silicon chip *Nature* 20014 431 1081-1084

[23] H. Rong et.al,. A continuous-wave Raman silicon laser *Nature* 2005 433 725-728

[24] A.I.Kuznetsov, et.al,. Roadmap for Optical Metsurfaces *ACS Photonics* 2024 doi 10.1021/acsphotonics.3c00457

[25] M. Higashiwaki, et.al,. Gallium oxide (Ga_2O_3) metal-semiconductor field-effect transistors on single-crystal β- Ga_2O_3 (010) substrates, *Appl Phys*. Let 2012 100 013504

[26] B.M. Janzen, et.al, Comprehensive Raman study of orthorhombic κ/ε- Ga_2O_3 and the impact of rotational domains *J. Mater Chem C* 2021 9 14175

[27] The growth of advanced semiconductor packaging | McKinsey and/or The Five Keys to Next-Generation IC Packaging Design: Part 1 - Semiconductor Packaging (siemens.com)

[28] Database of Raman spectroscopy, X-ray diffraction and chemistry of minerals (rruff.info)

Fran ADAR

Principle Raman Applications Scientist,
HORIBA Instruments Incorporated,
Ph.D.